# CHAPTER 42

## Measurement of Breaking Waves Using Particle Image Velocimetry

Kuang-An Chang [1] and Philip L.-F. Liu [2]

## 1. Introduction

The water wave breaking problem has been studied for many years. The most popular experimental methods for studying this problem include the flow visualization method and the Laser Doppler Velocimetry (LDV). However, the first method lacks quantitative description and the second method, in general, needs hundreds of measurements to form a flow field. Instantaneous quantitative flow field information is nearly impossible, if these two methods are used. In recent years, the Particle Image Velocimetry (PIV) has been proven to be a powerful tool for two-dimensional instantaneous velocity measurement. Tens to hundreds of velocity measurements using the LDV can be done in only one single measurement using the PIV.

The LDV is the most common tool for non-intrusive velocity measurements. By using the LDV and the phase average method, Mizuguchi (1986) and Okayasu et al.(1986) measured hundreds of points under a plunging breaker on sloping beaches. The flow fields of the mean and turbulence velocity were formed and the vorticity was calculated. In addition, Nadaoka et al. (1989) studied turbulent structures in surf zone using either the phase-averaged method or the moving-averaged method and demonstrated the differences between these two methods. In their work, the strain rate and its principal axes, Reynolds stress and momentum transport were obtained. More recently, a series of papers published by Ting and Kirby (1994, 1995, 1996) attempted to describe the turbulence structure under plunging and spilling breaking waves. In their works, turbulence transport under trough level was studied based on the turbulent kinetic energy equation. All the work mentioned above are based on either the phase or the moving average in turbulence measurements. In other words, experimental studies of wave breaking contain, in general, instantaneous and/or phase-averaged velocity information. As far as the authors know, the ensemble-averaged velocity field is rare for the unsteady problems such as breaking waves. However, the wave period in the

[1]Graduate Student, [2]Professor, School of Civil and Environmental Engineering, Cornell University, Ithaca, NY 14853

surf zone is not quite constant even for the monochromatically generated waves. The effect of the questionable "phase average" is not yet known.

Beside the LDV technique, the PIV has been used to measure velocity field in recent years. A good review of the PIV technique can be found in Adrian (1991). However, the PIV is still a quite new tool in water-wave related studies. A detailed description of the PIV used in a coastal engineering laboratory is given by Greated et al. (1992). By using PIV, Quinn (1995) studied near-breaking and broken waves on different slopes and compared the results with those of Boussinesq models. Skyner (1996) studied near-breaking plunging waves and compared PIV results with a boundary element model. The instantaneous flow field and the evolution of a quasi-steady breaking wave generated by a submerged airfoil was studied by Lin and Rockwell (1994, 1995). Hornung et al. (1995) measured velocity field and calculated vorticity under a hydraulic jump and used the results to confirm a control-volume prediction. Perlin et al. (1996) studied a plunging breaker in deep water and found the largest particle velocity is about 30% greater than the phase speed. In all the work mentioned above either the instantaneous flow field information or the quasi-steady breaker such as hydraulic jump was reported. No turbulence properties have been obtained.

In this study, deep-water spilling breaking waves are investigated by applying the PIV technique. By repeating the initial and boundary conditions carefully, the mean velocity and turbulence intensity are obtained from ensemble average.

## 2. Experimental Set-up

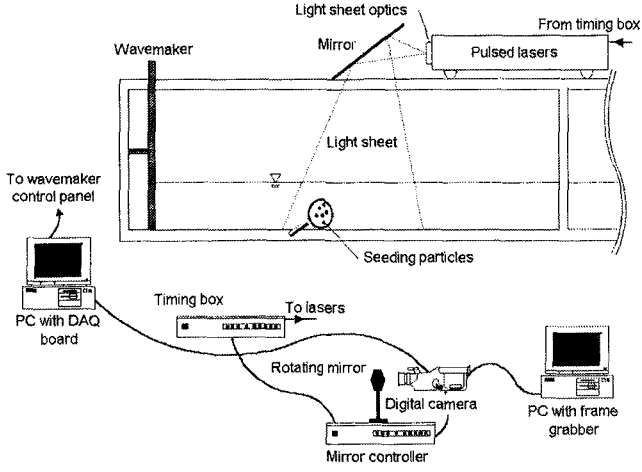


Figure 1: Experimental Set-up

The experiments were conducted in a 30m long, 0.6m wide and 0.9m deep wave tank. Waves are generated by a piston-type wavemaker controlled by a Pentium PC. Monochromatic waves were generated by moving the wave board periodically as fol-

lows: $\xi(t) = -A\cos(2\pi ft)$ in which $A = 7.0$ cm and $f = 1.0$ Hz. The error of the wave board motion is less than 0.5% of the stroke if the same motion is repeated. The PC also sent out pulses to trigger a camera so that the time interval between starting wavemaker and triggering camera can be well controlled. The breaking point, defined as the front face of wave becomes vertical, is about 1/3 of the wavelength away from the wave board at $x = 38$cm with $x = 0$ representing the center of wave board trajectory. The wavelength, calculated from linear theory, is 1.2m. A wave gauge placed close to breaking point at $x = 35$cm showed that the wave height is 14.5cm. The water depth was kept at 20cm. A light sheet about 1mm in thickness at the center of tank was created by frequency-doubled dual Nd:YAG lasers with a -12.7mm cylindrical lens combined with a 2000mm spherical lens. The lasers have a 200mJ/pulse maximum output energy and 10ns pulse duration in 532nm wavelength. A high resolution digital CCD camera (1316×1034 pixels) connected to a Pentium PC with a frame grabber in it was used to perform the so-called "on line" PIV. The camera equipped with a 60mm focus lens set at f/4.0 was located 2.7m in front of the light sheet. The field of view (FOV) is 40cm which is 1/3 of the wavelength and the resolution is 0.3mm/pixel. The time interval between two laser pulses was 2ms with error less than 1$\mu$s. In order to resolve the directional ambiguity, a rotating mirror was used (Adrian 1986). The lasers were located on top of the tank. The light sheet was redirected by a mirror to the test section. A black tape was stuck on the bottom of tank to reduce the reflection. The seeding particles were conifer pollen which has mean diameter 54$\mu$m and their specific weight are close to that of water. The conifer pollen has been proven to be good seeding particles for large scale PIV experiments (Greated et al. 1992). Velocity fields of three areas were measured. The first area is centered at $x$= 40cm where the wave starts to break. The second and the third area are centered at $x$= 70cm and $x$= 97cm, respectively, which are about 1/4 and 1/2 wavelength behind the breaking point. Only the results from the first and third measuring areas are shown here. The ensemble-averaged velocity was obtained by repeating 24 runs at the third measuring area for studying the turbulence generated by broken waves. See figure 1 for the sketch of experimental set-up.

After the image was captured, it was then analyzed by first applying the threshold to remove the noise and then performing the auto-correlation (Lourenco and Krothapalli 1994). The interrogation area for velocity calculation was 64×64 pixels. The timing was calibrated to have an uncertainty less than 1ms. Following the same procedure as the experiments were done, the error in velocity measurement is 1 cm/s which was obtained from the standard deviation of the stationary flow.

## 3. Results and Discussion

It is known that the particle velocity exceeds phase speed when a wave starts to break. This can be seen from figure 2 and 3. Figure 2 shows the velocity field under the second crest (first one doesn't break) just before breaking. The maximum velocity is 1.08 m/s which is 90% of the phase speed. Figure 3 shows the same wave crest just passing its breaking point. It has maximum velocity 1.52 m/s which is 25% greater than phase speed. Therefore it is expected that the particle velocity will be at least 25% higher than the phase speed during breaking.

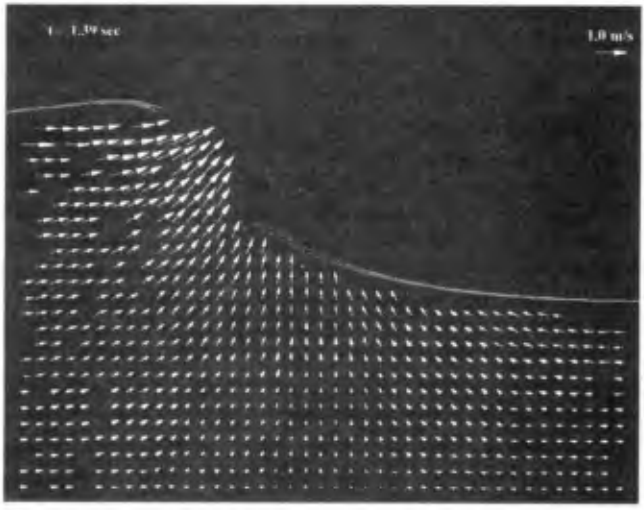

Figure 2: The first breaking wave reaching the breaking point at $t$ = 1.39 sec with FOV from $x$ = 21 to 61cm and $z$ = -17.4 to 14.4cm (the first measuring area).

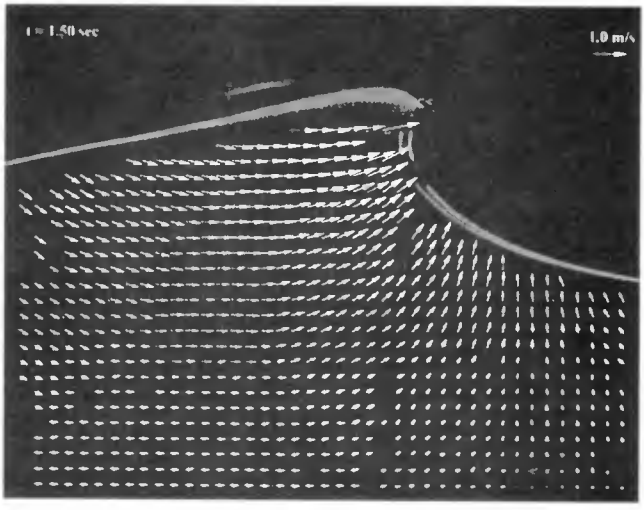

Figure 3: The first breaking wave passing the breaking point at $t$ = 1.50 sec with the same FOV as figure 2.

Once the wave breaks, it generates lots of air bubbles near the surface which make the measurement very difficult. Due to this reason, we only show velocity field at one particular moment– broken wave crest just passes the third measuring area. At this moment the area has the strongest turbulence and the measurements are not affected by air bubbles. In order to obtain turbulence intensity, 24 measurements with same boundary and initial conditions were taken. Figure 4(a) shows the instantaneous

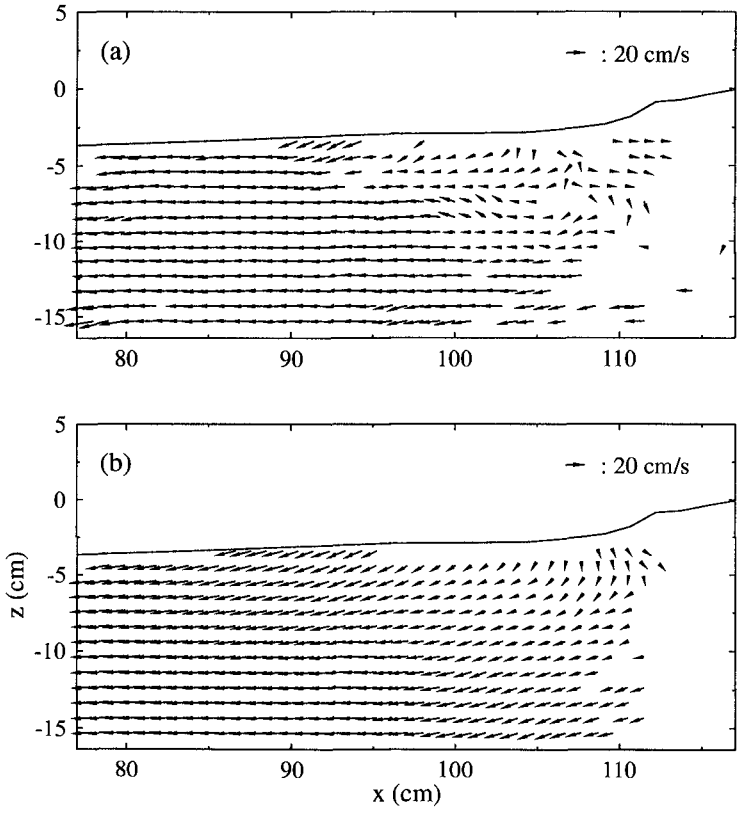


Figure 4: (a) Instantaneous velocity field (b) ensemble-averaged mean velocity field at $t$ = 3.39 sec with FOV from $x$ = 77 to 117cm and $z$ = -16.4 to 15.4cm (the third measuring area).

velocity field of one of the 24 measurements at the third measuring area centered at $x$ = 97cm which is about 1/2 wavelength behind the breaking point. Figure 4(b) shows the ensemble-averaged mean velocity from all 24 measurements. From the figure one

can see that some velocity data are missing near the right side. This is due to the residue air bubbles from the just-passed breaking waves. The linear kriging method (see Agterberg 1970) was used to interpolate and extrapolate the missing data. The

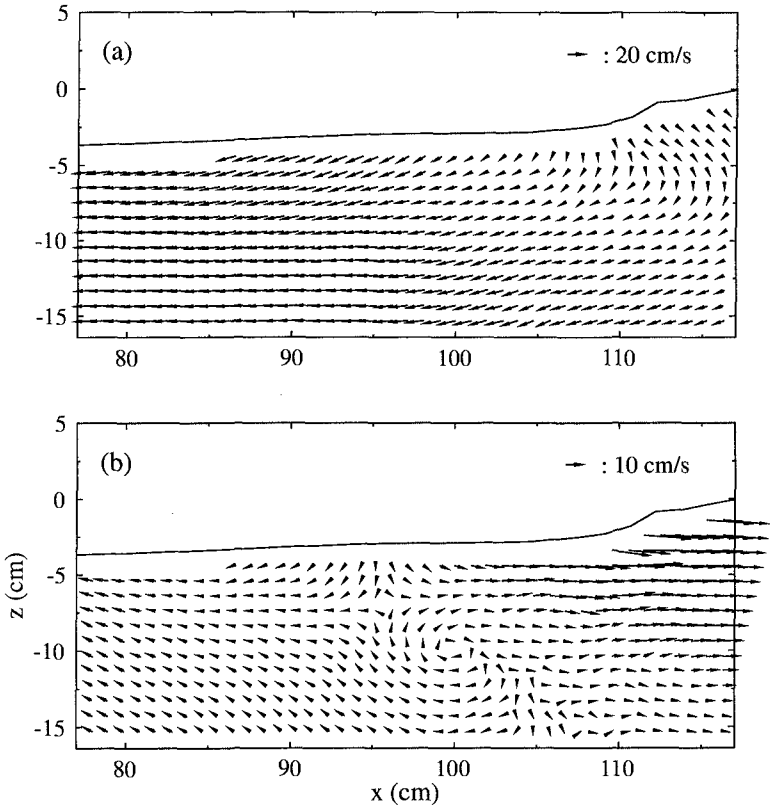


Figure 5: Linear kriging interpolated mean velocity field of figure 4(b) at (a) fixed frame (b) moving with (-0.2, -0.05)m/s.

interpolated velocity field is shown in figure 5(a). Figure 5(b) shows the same velocity field but from a moving frame (-0.2, -0.05)m/s. A clockwise vortex near the center of figure 5(b) can be clearly seen. This vortex is also shown in the later vorticity plot. Figure 6 shows the mean velocity contour in the horizontal and vertical directions. The vorticity of mean flow calculated by applying central finite difference is plotted in figure 7. One can find that the vorticity is negative in most of the area with the order of magnitude in a couple $sec^{-1}$. Figure 8 shows the turbulence intensity

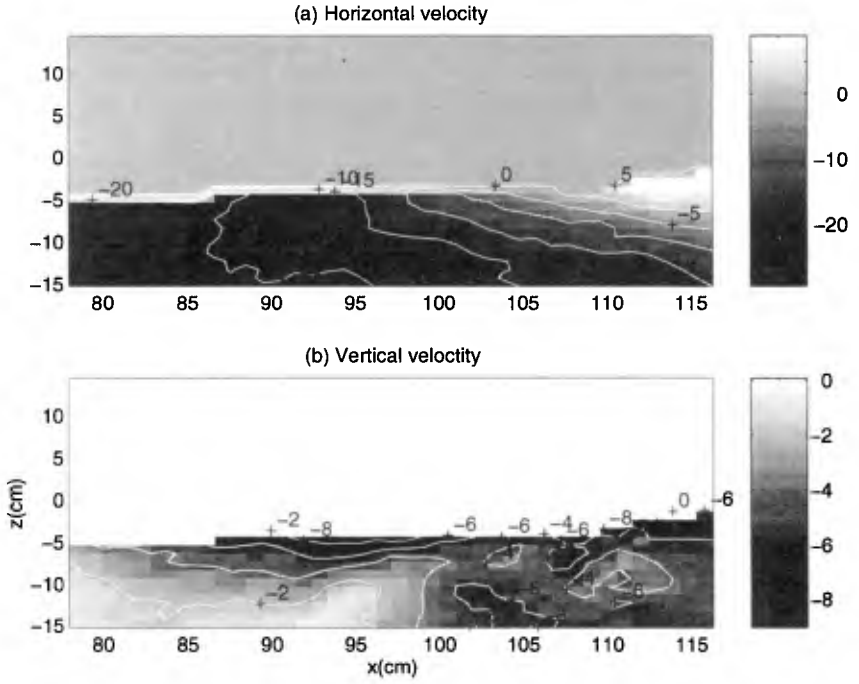


Figure 6: (a) Horizontal (b) vertical velocity (cm/s) of mean flow in the third measuring area.

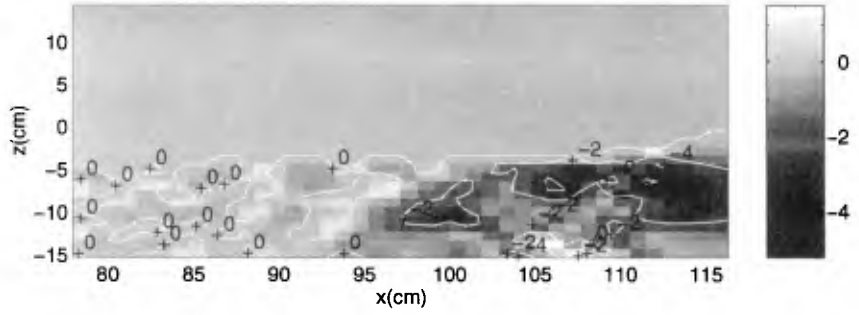


Figure 7: Vorticity (1/s) of mean flow in the third measuring area.

calculated from the ensemble average. Since the ensemble average is based on large number of samples, the ensemble-averaged turbulence intensity from different number of measurements were compared. It is found, from the contour plot, that the result from 15 measurements or more is close to that from 24 measurements. This may not mean 15 measurements are enough in performing ensemble average, but simply mean that the result from 15 measurements is quite close to that from 24 measurements and 15 measurements may be the minimum requirement. In other words, since it is difficult to obtain many measurements for calculating ensemble average in such kind of unsteady flow, at least 15 or more measurements may be necessary for performing the ensemble average. From figure 8 one can see the distribution of the turbulence

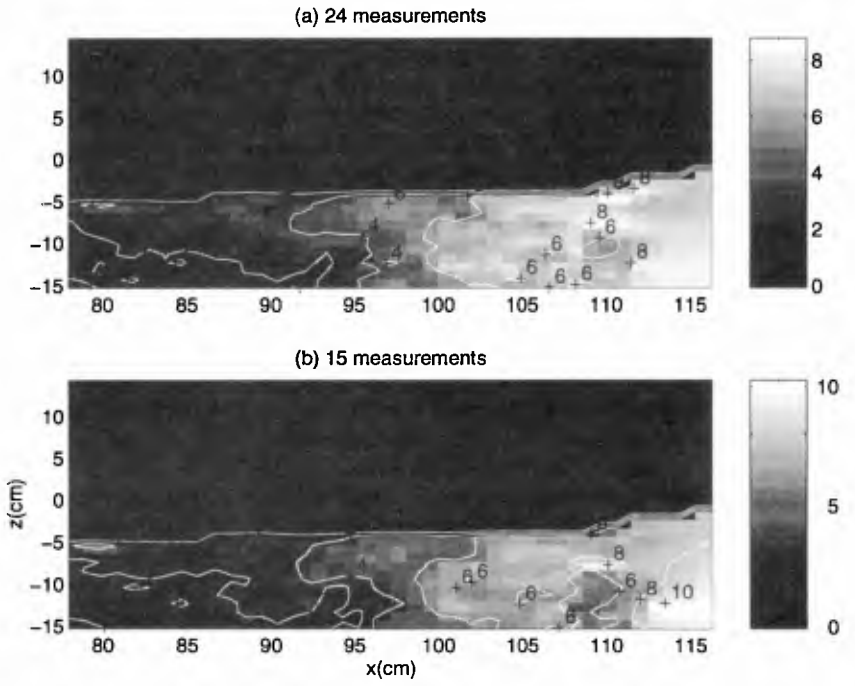


Figure 8: Turbulence intensity (cm/s) calculated from (a) 24 measurements (b) 15 measurements in the third measuring area.

intensity is quite uniform in the vertical direction. The maximum turbulence intensity in figure 8 is 10 cm/s. However, the maximum local mean velocity is only about 30 cm/s. This means that the turbulence intensity is almost the same order of magnitude as the local mean velocity, especially in the region close to the crest.

## 4. Conclusion

The PIV technique is proved to be a powerful tool in flow velocity measurement. The velocity field of non-breaking and near-breaking waves can be obtained without much difficulty. The maximum particle velocity of the deep-water spilling breaker is close to its phase speed at the breaking point and at least 25% greater than its phase speed during breaking. For broken waves, the mean velocity and turbulence intensity can be obtained from the ensemble average by repeating the same initial and boundary conditions. The turbulence intensity is about the same order of magnitude as the local mean velocity in the region the broken crest just passing through it. However, for the region which has highly concentrated air bubbles, more effort is needed in the future.

## Acknowledgement

This research was supported by a grant from the National Science Foundation (CTS-9302203) to Cornell University.

## References

Adrian, R. J. 1986 "Image shifting technique to resolve directional ambiguity in double-pulsed velocimetry." *Appl. Opt.*, **25**(21), 3855-3858.

Adrian, R. J. 1991 "Particle-imaging techniques for experimental fluid mechanics." *Annu. Rev. Fluid Mech.*, **23**, 261-304.

Agterberg, F. P. 1970 "Autocorrelation functions in geology." *Geostatistics*, Merriam, D.F. (ed.), 113-141.

Greated, C. A., Skyner, D. J. & Bruce, T. 1992 "Particle image velocimetry (PIV) in the coastal engineering laboratory." *Proc. 23th Int. Conf. Coastal Engrg.*, 212-225.

Hornung, H. G., Willert, C. & Turner, S. 1995 "The flow field downstream of a hydraulic jump." *J. Fluid Mech.*, **287**, 299-316.

Lin, J.-C. & Rockwell, D. 1994 "Instantaneous structure of a breaking wave." *Phys. Fluids*, **6**(9), 2877-2879.

Lin, J.-C. & Rockwell, D. 1995 "Evolution of a quasi-steady breaking wave." *J. Fluid Mech.*, **302**, 29-44.

Lourenco, L. & Krothapalli, A. 1994 "On the accuracy of velocity and vorticity measurements with PIV." *Experiments in Fluids*, **18**, 421-428.

Mizuguchi, M. 1986 "Experimental study on kinematics and dynamics of wave breaking." *Proc. Int. Conf. Coastal Engrg.*, 589-603.

Nadaoka, K., Hino, M. & Koyano, Y. 1989 "Structure of the turbulent flow field under breaking waves in the surf zone." *J. Fluid Mech.*, **204**, 359-387.

Okayasu, A., Shibayama, T. & Mimura, N. 1986 "Velocity field under plunging waves." *Proc. Int. Conf. Coastal Engrg.*, 660-674.

Perlin, M., He, J. & Bernal, L. P. 1996 "An experimental study of deep water plunging breakers." *Phys. Fluids*, **8**(9), 2365-2374.

Quinn, P. A. 1995 *Breaking Waves on Beaches.* PhD thesis, University of Edinburgh.

Skyner, D. 1996 "A comparison of numerical predictions and experimental measurements of the internal kinematics of a deep-water plunging wave." *J. Fluid Mech.*, **315**, 51-64.

Skyner, D. J., Gray, C. & Greated, C. A. 1990 "A comparison of time-stepping numerical predictions with whole-field flow measurement in breaking waves." *Water Wave Kinematics*, eds. A. Torum and O.T. Gudmestad, 491-508.

Ting, F.C.K. & Kirby, J. T. 1994 "Observation of undertow and turbulence in a laboratory surf zone." *Coastal Engineering*, **24**, 51-80.

Ting, F.C.K. & Kirby, J. T. 1995 "Dynamics of surf-zone turbulence in a strong plunging breaker." *Coastal Engineering*, **24**, 177-204.

Ting, F.C.K. & Kirby, J. T. 1996 "Dynamics of surf-zone turbulence in a strong spilling breaker." *Coastal Engineering*, **27**, 131-160.